Research in Pharmaceutical Sciences, February 2025; 20(1): 142-164
Received: 21-10-2024
Peer Reviewed:12-11-2024
Revised: 31-01-2025
Accepted: 02-02-2025
Published: 20-02-2025

School of Pharmacy & Pharmaceutical Sciences
Isfahan University of Medical Sciences

Original Article

Synthesis and *in vitro* evaluation of self-assembling biocompatible heparin-based targeting polymeric micelles for delivery of doxorubicin to leukemic cells

Jaber Emami[1], Moloud Kazemi[2,3,*], and Mina Mirian[4]

[1]*Department of Pharmaceutics, School of Pharmacy and Pharmaceutical Sciences, Isfahan University of Medical Sciences, Isfahan, I.R. Iran.*
[2]*Nanotechnology Research Center, Medical Basic Research Sciences Institute, Ahvaz Jundishapur University of Medical Sciences, Ahvaz, Iran.*
[3]*Department of Pharmaceutics, Faculty of Pharmacy, Ahvaz Jundishapur University of Medical Sciences, Ahvaz, Iran.*
[4]*Department of Pharmaceutical Biotechnology, School of Pharmacy and Pharmaceutical Sciences, Isfahan University of Medical Sciences, Isfahan, I.R. Iran.*

Abstract

Background and purpose: Biodegradable polymeric micelles have emerged as one of the most promising platforms for targeted drug delivery. In the present study, a polymeric micelle composed of folic acid (FA), heparin (HEP), dexamethasone (DEX), and (FA-PEG-HEP-CA-TOC) was developed for the delivery of doxorubicin (DOX) to leukemic cells.

Experimental approach: FA-HEP-DEX was synthesized and characterized by ^{1}H-NMR. DOX-loaded micelles were prepared using a dialysis method. The impact of various processing variables, including polymer-to-drug ratio, dialysis temperature, and solvent type, on the physicochemical properties of the micelles were evaluated. In vitro, cellular uptake and cytotoxicity of the micelles in folate receptor-positive (K562) and negative (HepG2) cells were evaluated.

Findings/Results: The ^{1}H-NMR results confirmed the successful synthesis of FA-HEP-DEX. DOX-loaded micelles exhibited an average particle size of 117 to 181 nm with a high drug entrapment efficiency (36% to 71%). DOX-loaded micelles also showed sustained drug-release behavior. DOX-loaded FA-HEP-DEX micelles exhibited higher cellular uptake and *in vitro* cytotoxicity than free DOX and DOX-loaded HEP-DEX micelles in K562 cells.

Conclusions and implications: DOX was well incorporated into the micelles with high entrapment efficiency due to high solubility of DOX in DEX as the hydrophobic component of the micelle structure. The higher cellular uptake and cell toxicity of targeted micelles correspond to the presence of FA on the micelle surface, which promotes cell internalization of the micelles *via* specific receptor-mediated endocytosis. Our results indicated the potential of DOX-loaded heparin-based micelles with desirable antitumor activity as a targeted drug delivery system in cancer therapy.

Keywords: Dexamethasone; DOX; Heparin; Leukemia; Polymeric micelle.

INTRODUCTION

Leukemia is a hematopoietic stem cell malignancy and the 10th most prevalent type of cancer worldwide (1,2). It is characterized by an accumulation of immature, undifferentiated blast cells in the blood and bone marrow (3). Leukemia can be divided into lymphoid or myeloid lineages, and further classified as acute or chronic based on the maturity of the cells. The hallmark of leukemia is the uncontrolled proliferation of leukemic blast cells that exhibit poor differentiation. The main treatment strategies rely on anthracycline-based chemotherapy, which can induce complete remission in around 70% of leukemic patients.

*Corresponding author: M. Kazemi
Tel: +98-9393482621, Fax: +98-6133110000
Email: mk.pharm68@gmail.com

Access this article online	
	Website: http://rps.mui.ac.ir
	DOI: 10.4103/RPS.RPS_197_24

Doxorubicin (DOX), an effective anthracycline chemotherapy agent, is widely used in treating solid tumors and hematological cancers (4). However, the efficacy of DOX in cancer therapy is limited by dose-dependent side effects such as myelosuppression and cardiotoxicity. Dose-dependent cardiac toxicity is a major adverse effect of DOX that can impair patient outcomes and survival (5). The mechanism underlying DOX's early cardiotoxic effects is partly related to free radical injury, where DOX forms complexes with iron, leading to reactive oxygen species formation, intracellular damage, and cardiomyocyte death (6-11). Mitochondrial DNA mutations have also been implicated as a possible mechanism for the delayed cardiotoxicity observed in long-term survivors, though the causes are multifactorial. These cardiotoxic pathways appear distinct from DOX's primary anticancer mechanism of DNA topoisomerase II inhibition (12,13).

DOX rapidly and selectively decreases the expression of cardiac α-actin, as well as other muscle genes like cardiac troponin I and myosin light chain 2, in cultured cardiomyocytes. These changes represent some of the earliest manifestations of DOX cardiomyopathy (14) and precede the characteristic ultrastructural alterations induced by DOX toxicity (15). This provides researchers with an experimental model to evaluate the effects of synthetic glucocorticoids, such as dexamethasone (DEX), on DOX-induced cardiotoxicity in embryonic stem cell-derived cardiomyocytes.

Glucocorticoids were among the first drug classes used for the treatment of patients with acute lymphoblastic leukemia (ALL) and remain essential components of therapy. They exert cytotoxic effects by binding to glucocorticoid receptors in the cytoplasm. These receptors can dimerize, translocate to the nucleus, and interact with glucocorticoid response elements to activate gene expression. Alternatively, the receptors can remain as monomers and repress the activity of transcription factors like activating protein-1 (AP-1) or nuclear factor-κB (NFκB). Both pathways inhibit cytokine production, alter oncogene expression, and induce cell cycle arrest and apoptosis (16).

DEX, a glucocorticoid steroid hormone, is widely utilized as a potent anti-inflammatory agent and regulator of bone growth. DEX is also one of the most commonly used chemotherapeutic drugs for treating childhood leukemia. It induces apoptosis in B and T lymphocytes, consequently killing a large population of leukemic cells.

The advantages of DEX over prednisone include its 5.5 to 16 times greater antileukemic activity and enhanced penetration into cerebrospinal fluid with a longer half-life. This results in decreased central nervous system relapse. DEX also exhibits an anti-inflammatory potency around nine times higher than prednisolone.

However, long-term systemic exposure to DEX causes adverse side effects including fluid retention, growth retardation, gastrointestinal bleeding, joint damage leading to pain and osteoporosis, hyperglycemia, hypertension, increased ocular pressure, and most critically, immunosuppression due to nonspecific prevention of proliferation of normal T and B lymphocytes (17).

Among the drug combinations used for the initial treatment of multiple myeloma, DEX and DOX are the most widely combined to improve response rates compared to earlier regimens. However, administering these drugs requires 96-h continuous infusion through a central venous catheter due to their poor water solubility. This necessitates hospitalization in many patients and may increase infection risk. Moreover, the high corticosteroid doses needed with this regimen can cause substantial toxicity (17). Therefore, developing a new delivery system for these two poorly water-soluble drugs has been greatly needed. We, therefore, aimed to develop a novel drug delivery system for the combinatorial delivery of DEX and DOX.

A water-soluble polysaccharide, heparin (HEP), with favorable biocompatibility, biodegradability, and biological activity was conjugated with the poorly water-soluble DEX. This resulted in an amphiphilic polysaccharide-based prodrug capable of self-assembling into spherical polymeric micelles in aqueous environments (18). The amphiphilic copolymer was then modified with folic acid (FA) as a targeting ligand (19,20). Using these micelles, the hydrophobic base of DOX was incorporated

into their hydrophobic cores. The *in vitro* physicochemical properties, cytotoxicity, and intracellular accumulation of the DOX-loaded micelles were investigated in human erythroleukemic (K562) cells.

MATERIALS AND METHODS

Materials

Enoxaparin sodium (MW, 4 KDa) from Iran Hormone Company (Iran), DOX from the Indian Pharmaceutical and Biotechnology Company (India), DEX, triethylamine (TEA), dicyclohexylcarbodiimide (DCC), 4-dimethylaminopyridine (DMAP), N-(3-dimethyl-aminopropyl)-carbodiimide hydrochloride (EDCI), N-hydroxysuccinimide (NHS), polyethylene glycol-bis-amine (MW: 3 KDa), pyrene, FA and dialysis bag (molecular weight cut-off, MWCO: 2 KDa) from Sigma-Aldrich Company (Germany); tetrahydrofuran (THF), formamide, dimethylformamide (DMF) from Samchun Company (South Korea); anhydrous dimethyl sulfoxide (DMSO), acetone, methanol, potassium phosphate dibasic, and sodium hydroxide from Merck Company (Germany); trypsin and phosphate buffer saline (PBS) from BIO-IDEA (USA, New York).

Cell lines and culture conditions

Human erythroleukemic (K562) and human liver hepatocellular carcinoma (HepG2) cell lines were supplied by the Pasteur Institute of Iran (Iran, Tehran). K562 and HepG2 cells were incubated in Dulbecco's modified eagle's medium (DMEM, BIO-IDEA, USA, New York) and Roswell Park Memorial Institute medium (RPMI 1640, BIO-IDEA, USA, New York), respectively. Culture media were supplemented with 10% fetal bovine serum (FBS; BIO-IDEA, USA, New York) and 1% antibiotics containing 100 U/mL penicillin and 100 µg/mL streptomycin (Gibco Laboratories USA, New York). The cells were cultured at 37 ℃ in a humidified atmosphere with 5% CO_2.

Synthesis of amphiphilic copolymer

Synthesis of HEP-DEX copolymer

DEX was conjugated to HEP through the DCC/DMAP coupling reaction based on previous studies with minor modifications (21). Briefly, HEP (0.05 mmol) dissolved in anhydrous formamide with gentle heating. DCC (0.15 mmol) and DMAP (0.15 mmol) already dissolved in anhydrous DMF were added to the flask and stirred for 2 h at room temperature under a nitrogen atmosphere. Afterward, DEX (0.3 mmol) was dissolved in anhydrous DMF and then added to the reaction mixture which was continued for 48 h at room temperature. The reaction mixture was then filtered to remove any 1,3-Dicyclohexyl urea (DCU) byproducts and then precipitated with excess cold acetone. The resulting precipitate was centrifuged and washed twice with acetone. To remove unreacted material, the precipitate was dialyzed against methanol for 48 h followed by water for another 24 h using dialysis membranes (MWCO: 2 KDa) which were then lyophilized to obtain the HEP-DEX pure powder (freeze dryer Model ALPHA 2-4 LD plus, Christ Company, Stuttgart, Germany).

Synthesis of amine-terminated folate (FA-NH_2)

Amine-terminated folate (FA-NH_2) was synthesized according to the study of Li *et al.* (22). Briefly, FA (0.15 mmol) dissolved in DMSO was reacted with EDC (0.3 mmol) and NHS (0.3 mmol) in a dark flask at room temperature for 12 h under nitrogen gas by activating the FA carboxyl group. The resulting activated folate-NHS was reacted with ethylenediamine (0.3 mmol) and pyridine (100 µL) in the dark at room temperature for another 24 h. The FA-NH_2 was precipitated in the excess acetonitrile, washed with diethyl ether three times, and then dried under a vacuum to obtain the yellow powder.

Synthesis of FA-HEP-DEX co-polymer

FA-NH_2 was conjugated to HEP-DEX by an amidation reaction between the carboxyl group of HEP and the free amine group of FA-NH_2. HEP-DEX (0.05 mmol), EDC (0.15 mmol), and NHS (0.15 mmol) were dissolved in anhydrous DMSO and stirred for 2 h under the protection of nitrogen. Afterward, FA-NH_2 (0.15 mmol) was added to the mixture and the reaction was continued for 72 h at room temperature. After that, the product was precipitated by a large volume of acetone, then centrifuged (3000 rpm) and washed twice. For further purification, the precipitate was dialyzed against methanol for 48 h followed by water for 24 h, and then lyophilized.

HEP-DEX and FA-HEP-DEX characterization

Synthesis of HEP-DEX and FA-HEP-DEX copolymers was confirmed using ^{1}H-nuclear magnetic resonance (^{1}H-NMR; Bruker Biospin, 400 MHz, Germany). For ^{1}H-NMR characterization, the copolymers were dissolved in DMSO-d_6:D_2O (1:4), DEX and FA were dissolved in DMSO-d_6, and HEP was dissolved in D_2O before measurement.

Determination of critical micelle concentration

The critical micelle concentration (CMC) of HEP-DEX and FA-HEP-DEX was determined by fluorescence spectroscopy using pyrene as a hydrophobic fluorescence probe (21). Briefly, a pyrene solution in acetone at a fixed concentration (5×10^{-6} mol/L) was added to a series of 10-mL glass tubes, then the solvent was evaporated under a stream of nitrogen gas. Afterward, polymer solutions at concentrations ranging from 1 to 200 µg/mL were added to each tube to obtain a final pyrene concentration of 5×10^{-7} mol/L. The mixtures were shaken at 37 °C for 24 h in a dark room. The fluorescence emission spectra of pyrene in the polymer solutions were recorded using a spectrofluorometer (Jasco FP 750, Tokyo, Japan) with the excitation wavelength set at 336 nm. For the pyrene emission spectra, the intensity ratios of the first peak (I_1, 374 nm) to the third peak (I_3, 390 nm) were plotted against the logarithm of the polymer concentration. Two tangents were then drawn and the CMC value was taken from the intersection between the two tangents.

Micelle fabrication and experimental design

DOX-loaded FA-HEP-DEX micelles were prepared by a dialysis technique as reported in previous studies (22). Briefly, FA-HEP-DEX copolymer was dissolved in water. DOX was dissolved in two different organic solvents (DMF or THF) and then deprotonated by adding triethylamine in an equivalent molar ratio to obtain hydrophobic DOX. Afterward, the DOX solution was added dropwise to the polymer solution at two different polymers-to-drug ratios (P/D, 2 or 5) under ultrasonication (JY 92-II Ultrasonic Processor, Shanghai, China) for 10 min in an ice bath. The mixture was stirred for 30 min and then dialyzed against water for 12 h at two different temperatures (25 °C or 45 °C) to remove the organic solvent. After that, the obtained micelle dispersion was centrifuged at 3000 rpm for 10 min and the supernatant was filtered through a 0.45 µm pore size microfilter to remove free un-encapsulated drug and then freeze-dried. The lyophilized drug-loaded micelles were collected and kept at 4 °C until further evaluation. Polymeric micelle formulations generated by Design Expert® 7 using a full factorial design are listed in Table 1.

Determination of drug content in polymeric micelles

An appropriate amount of the lyophilized DOX-loaded polymeric micelle was dissolved in DMF, sonicated for 10 min and filtrated. The concentration of encapsulated DOX in the resulting solution was then determined using a UV-visible spectrophotometer (Biochrom WPA BioWave II, England) at 480 nm. To investigate potential interactions among the formulation components in determining the drug amount, the maximum wavelength was measured once for the drug-free nanoparticles and once for the drug alone. Additionally, a blank sample without the drug was prepared from all formulations, which was used for calibrating the device in the quantification tests.

Table 1. Proposed formulations by Design Expert®7for the evaluation of doxorubicin-loaded micelles using the full factorial design

Formulation	Polymer/drug	Temperature (℃)	Solvent type
$T_{25}P_2F$	2	25	DMF
$T_{25}P_5F$	5	25	DMF
$T_{45}P_2F$	2	45	DMF
$T_{45}P_5F$	5	45	DMF
$T_{25}P_2H$	2	25	THF
$T_{25}P_5H$	5	25	THF
$T_{45}P_2H$	2	45	THF
$T_{45}P_5H$	5	45	THF

The entrapment efficiency (EE) and loading content (LC) were calculated using the following equations:

$$EE\ (\%) = \frac{Weight\ of\ the\ drug\ in\ the\ micelles}{Weight\ of\ the\ feeding\ drugs} \times 100 \quad (1)$$

$$LC\ (\%) = \frac{Weight\ of\ the\ drug\ in\ the\ micelles}{Weight\ of\ the\ micelles} \times 100 \quad (2)$$

Particle size and zeta-potential measurement

The particle size (PS), polydispersity index (PDI), and zeta potential (ZP) of the polymeric micelles in aqueous media were measured by dynamic light scattering (DLS) at 25 ℃ utilizing Malvern Zetasizer Nano-ZS (Malvern Instruments Ltd., UK).

In vitro drug release studies

In vitro release of DOX from the polymeric micelles was carried out in PBS (0.01 M) using a dialysis method. One mL of DOX-loaded polymeric micelles was introduced into a dialysis bag (MW cutoff: 6-8 KDa) and immersed in a release medium at 37 ℃ with agitation to provide sink conditions. At predetermined time intervals, 1 mL aliquots of the release medium were withdrawn to determine the drug concentration and replaced with an equal volume of fresh medium (22). The concentration of DOX in the samples was quantified by UV-visible spectroscopy (Biochrom WPA BioWave II, England) at 480 nm. Based on the release profiles, the mean drug release time (MDRT) was calculated using the following equation (23):

$$\mathrm{MDRT(h)} = \frac{\sum_{i=1}^{n} t_{mid}\,\Delta M_i}{\sum_{i=1}^{n} \Delta M_i} \quad (3)$$

where, i is the sampling number; n is the last sampling number; t_{mid}, the time at the midpoint between t_i and t_{i-1} (calculated as $(t_i + t_{i-1})/2$); and ΔM_i is the additional amount of drug released between t_i and t_{i-1}.

Optimization

The optimization was carried out by the Design Expert®7 using a computer optimization process. The optimized formulation was then prepared in the laboratory, and all the dependent variables were determined practically. Based on the predicted and actual responses, the error percent was calculated.

Morphological evaluation of the optimized micelles

The morphology and shape of the optimized micellar formulation were observed under transmission electron microscopy (TEM; LEO 906 E, Germany) with an accelerating voltage of 80 kV.

Cellular uptake studies

A qualitative cellular uptake examination of DOX-loaded micelles was evaluated using a fluorescence microscope (Nikon, Eclipse Ti-U, Japan). K562 (folate receptor positive) and HepG2 (folate receptor negative) cells were seeded into a 6-well plate at 2×10^5 cells per well in 1 mL of growth medium and incubated for 24 h for cell attachment (HepG2 cells). K562 cells growing in suspension were collected after 24 h of incubation.

Thereafter, the cells were treated with free DOX solution or DOX-loaded micelles (targeted and non-targeted) and incubated for 4 h and cells were washed with PBS (pH 7.4, 10 mM) and directly observed by fluorescent microscope.

To quantitatively assay cellular uptake, K562 and HepG2 cells were seeded at a density of 5×10^5 cells per well in a 6-well plate and incubated for 24 h. After 24 h, the cells were treated with either a free DOX solution or DOX-loaded micelles and incubated for 4 h. The cells were then washed with PBS, trypsinized, and harvested by adding 1 ml of PBS followed by 2 min ultrasonication at room temperature to obtain the cell lysate. Finally, the cell lysate was centrifuged at 10000 rpm for 10 min and the supernatant was used for fluorescence assay using a spectrofluorometer (Jasco FP-750, Tokyo, Japan) with excitation at 480 nm and emission at 560 nm. The cellular uptake of DOX was calculated using the following equation:

$$Cellular\ uptake\ perccentage\ of\ fluorescent\ micelles = \frac{I}{I_0} \times 100 \quad (4)$$

where I is the fluorescence intensity at different times and I_0 is the initial fluorescence intensity of the fluorescent micelles.

In vitro cytotoxicity assay

The *in vitro* cytotoxicity studies were conducted against K562 cells which show over-expressed folate receptors, and HepG2 cells which express folate receptors at undetectable levels using MTT assay.

The cells were seeded in 96-well plates at a density of 2×10^4 cells per well and incubated for 24 h. Afterward, the cells were exposed to various formulations (free DOX, DOX/HEP-DEX, or DOX/FA-HEP-DEX) at DOX concentrations ranging from 0.01-10 µM and incubated for 48 and 72 h. Cytotoxicity of HEP-DEX and FA-HEP-DEX micelles (blank micelles) was evaluated at the same micelle quantity as those of DOX-loaded formulations. After incubation time, 20 µL of MTT solution (5 mg/mL in PBS) was added to each well, followed by incubation for another 4 h. After that, the medium containing unreacted MTT was discharged and the formazan crystals were dissolved by 150 µL of DMSO. The absorbance values of the solution in each well were measured at 570 nm using an ELISA reader (Star Fax-2100, Awareness, Palm City, FL). Untreated cells were used as the negative control with 100% viability. Cell viability for each sample was calculated using the following equation:

$$Cell\ viability\ (\%) = \frac{Mean\ absorbance\ of\ each\ group - mean\ absorbance\ of\ the\ blank}{Mean\ absorbance\ of\ the\ negative\ control - mean\ absorbance\ of\ the\ blank} \times 100 \quad (5)$$

Folate competition assay

To confirm the findings of the selective targeting of folate receptors on K562 cells by folate-targeted DOX/FA-HEP-DEX and non-targeted DOX/HEP-DEX micelles, a competitive experiment was carried out. Here, free folic acid within the concentration range of 0 - 1000 µg/mL was added to each well 30 min before the addition of micellar formulation. The viability of the cells was then quantified, as described in the earlier section.

Statistical analysis

Data are expressed as mean ± SD of three separate experiments. Comparison of statistical data was conducted by Students t-test for two groups and one-way ANOVA for multiple groups followed by Tukey's post hoc test. *P*-values less than 0.05 were considered statistically significant in all cases.

RESULTS

Synthesis of HEP-DEX and FA-HEP-DEX

The chemical structure and synthesis pathways of FA-HEP-DEX are shown in Fig. 1.

Characterization of FA-HEP-DEX copolymer

The synthesized copolymer structure was confirmed by ^{1}H-NMR. Related ^{1}H-NMR spectra are shown in Fig. 2.

CMC determination of amphiphilic copolymers

Amphiphilic copolymer could form in the micelle in aqueous medium due to the hydrophobic interaction of the inner core. The CMC values of folate-targeted copolymers were determined using pyrene as a fluorescence probe. Figure 3 shows the fluorescence intensity ratio (I_1/I_3) versus the logarithm of polymer concentration. The CMC was obtained from the intersection of the two tangents in the curve of the intensity ratio of I_1/I_3 versus the logarithm of polymer concentration. The CMC values of FA-HEP-DEX and HEP-DEX were 4.206 and 1.806 µg/mL, respectively.

Physicochemical properties of micellar formulation

A summary of the physicochemical properties of the designed polymeric micelle formulations is represented in Table 2.

Optimization

The optimized formulation was chosen based on the criteria to achieve the smallest PS and maximum EE. The optimized formulation with a desirability factor of 0.75 with the suggested variable levels at 3.35 for P/D, 45 for temperature, and DMF as a solvent was prepared and then evaluated for PS, EE, loading percent (LP), ZP, and MDRT. The predicted and observed values of the dependent variables as well as the percentage of prediction error are shown in Table 3.

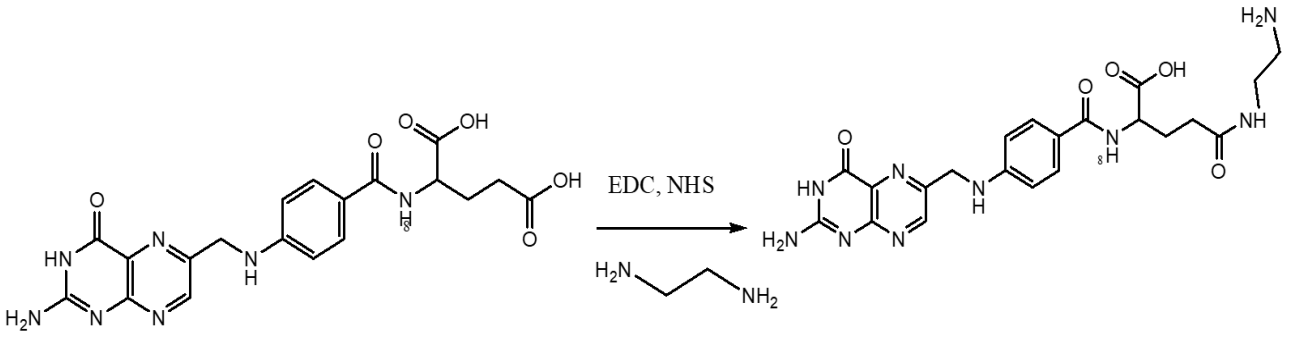

FA EDA FA-EDA

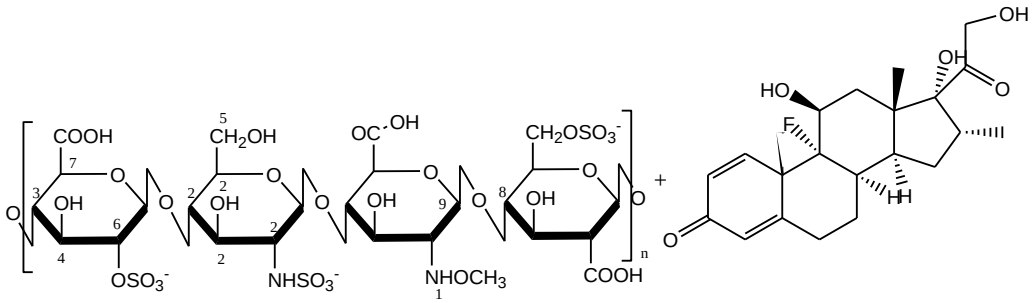

HEP DEX

DCC, DMAP

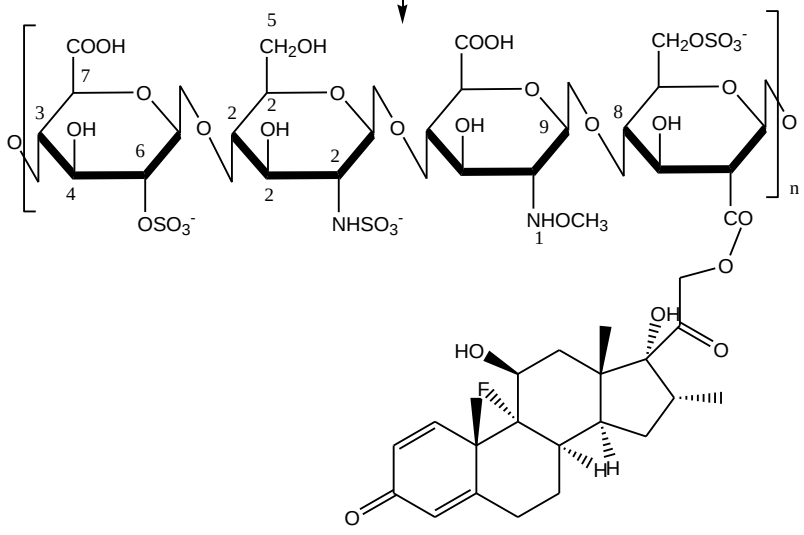

HEP-DEX

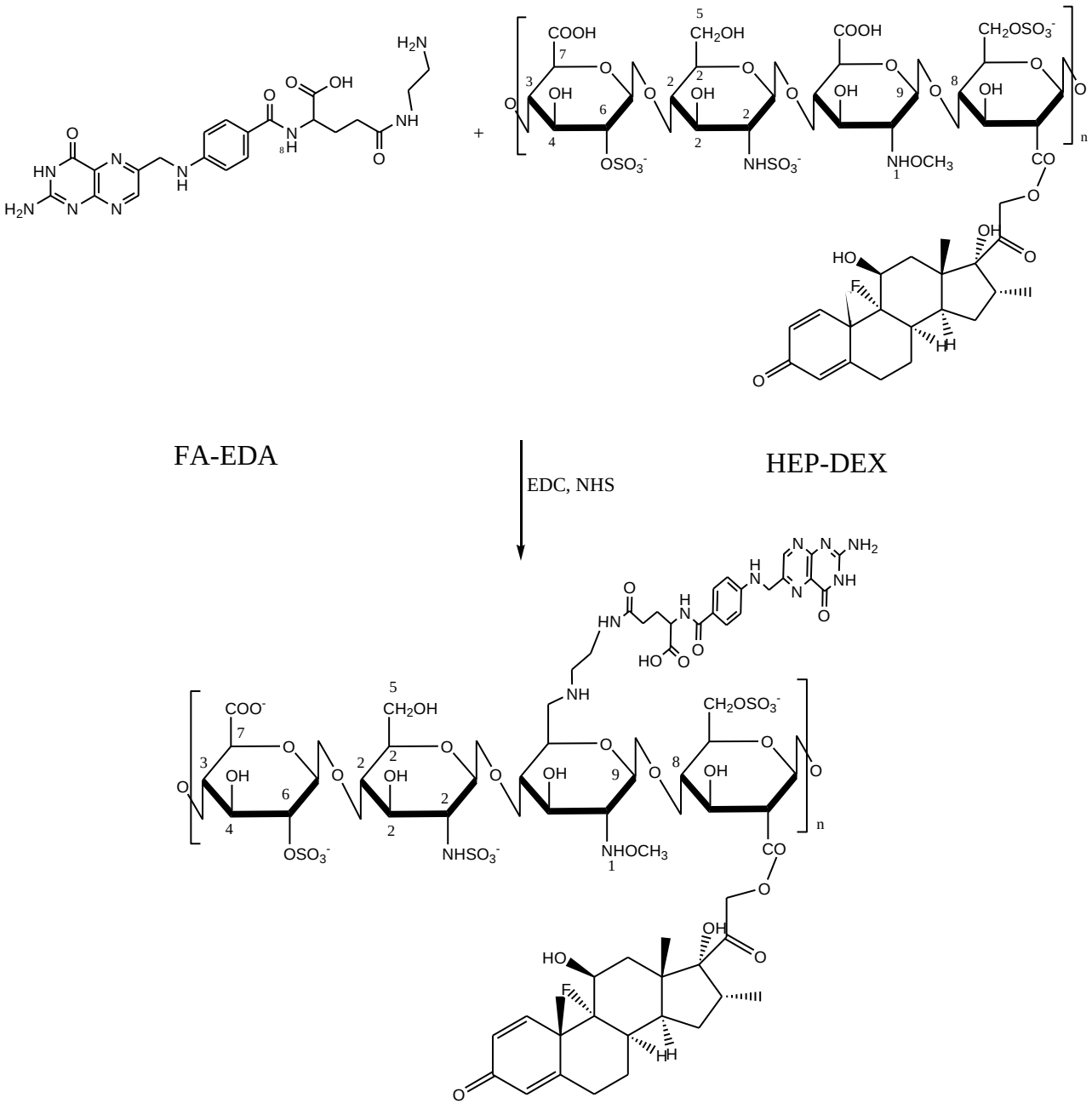

Fig. 1. Schematic presentation of FA-HEP-DEX conjugate synthesis. FA, Folic acid; HEP, heparin; DEX, dexamethasone; EDA, ethylene diamine; EDC, N-(3-dimethylaminopropyl)-carbodiimide hydrochloride, NHS, N-hydroxysuccinimide; DCC, dicyclohexylcarbodiimide; DMAP, 4-dimethylaminopyridine.

A

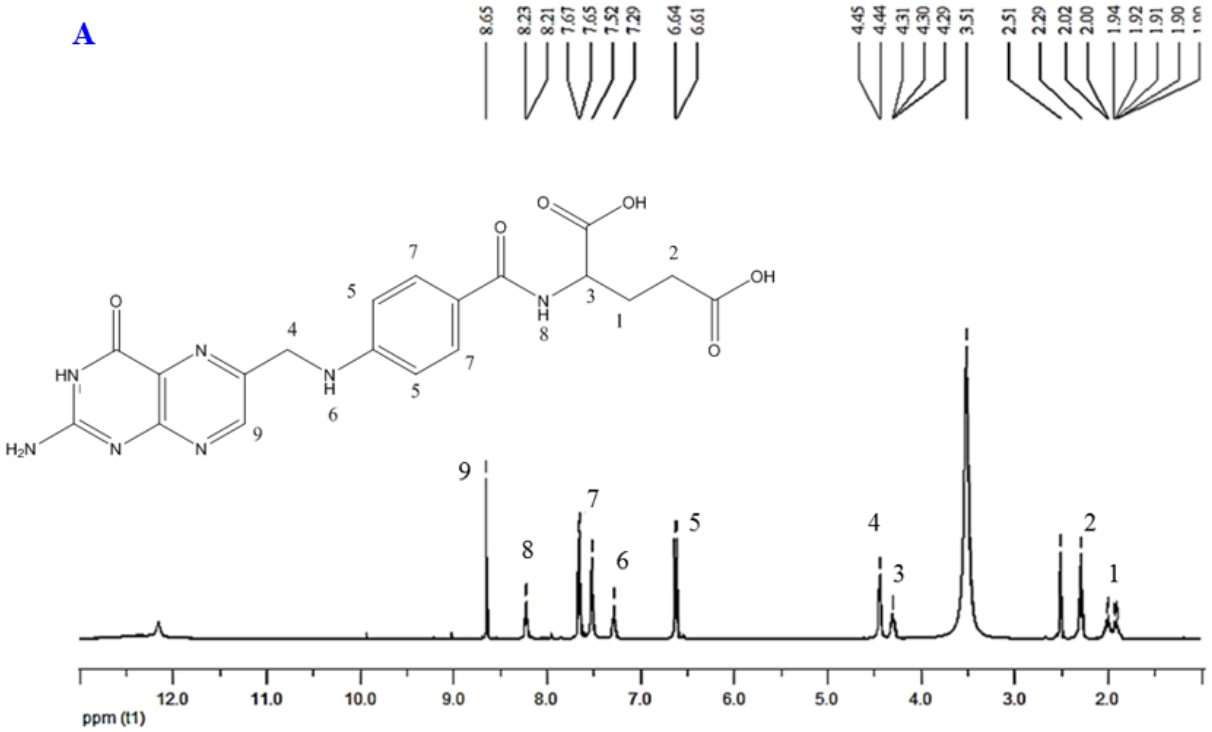
8.65
8.23
8.21
7.67
7.65
7.52
7.29
6.64
6.61
4.45
4.44
4.31
4.30
4.29
3.51
2.51
2.29
2.02
2.00
1.94
1.92
1.91
1.90
OH
OH
HN
H_2N
N
N
N
N
H
H
O
O
O
O
9
8
7
6
5
4
3
2
1
12.0
11.0
10.0
9.0
8.0
7.0
6.0
5.0
4.0
3.0
2.0
ppm (t1)

B

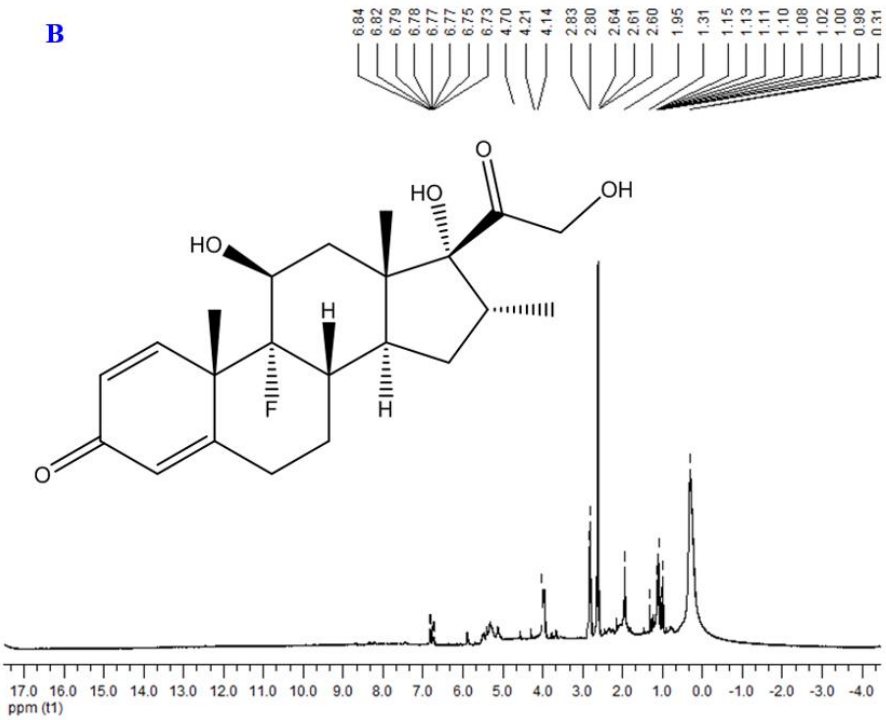
6.84
6.82
6.79
6.78
6.77
6.77
6.75
6.73
4.70
4.21
4.14
2.83
2.80
2.64
2.61
2.60
1.95
1.31
1.15
1.13
1.11
1.10
1.08
1.02
1.00
0.98
0.31
HO
HO
OH
O
O
H
H
H
17.0
16.0
15.0
14.0
13.0
12.0
11.0
10.0
9.0
8.0
7.0
6.0
5.0
4.0
3.0
2.0
1.0
0.0
-1.0
-2.0
-3.0
-4.0
ppm (t1)

C

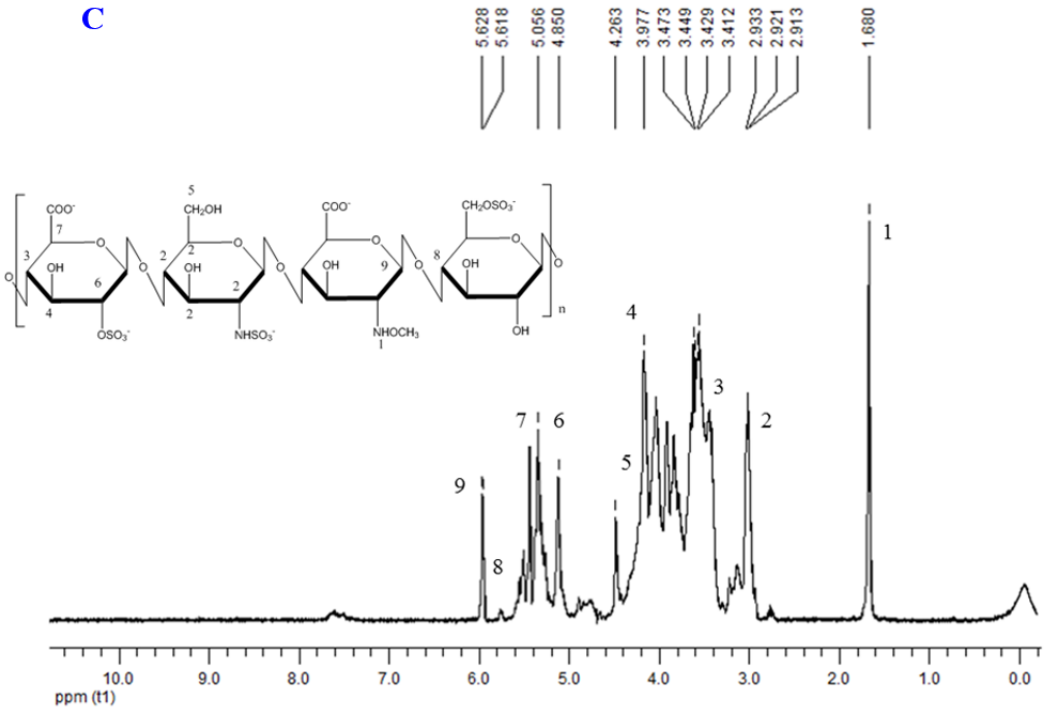
5.628
5.618
5.056
4.850
4.263
3.977
3.473
3.449
3.429
3.412
2.933
2.921
2.913
1.680
1
2
3
4
5
6
7
8
9
ppm (t1)

D

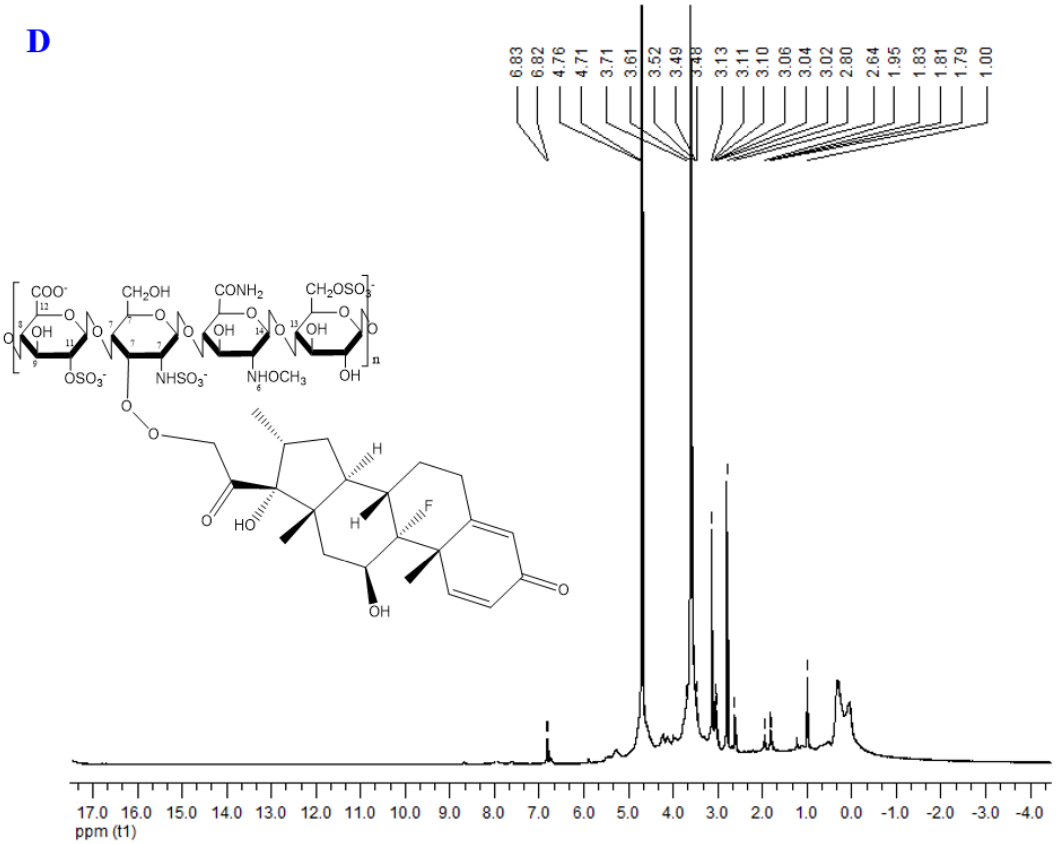
6.83
6.82
4.76
4.71
3.71
3.61
3.52
3.49
3.48
3.13
3.11
3.10
3.06
3.04
3.02
2.80
2.64
1.95
1.83
1.81
1.79
1.00
ppm (t1)

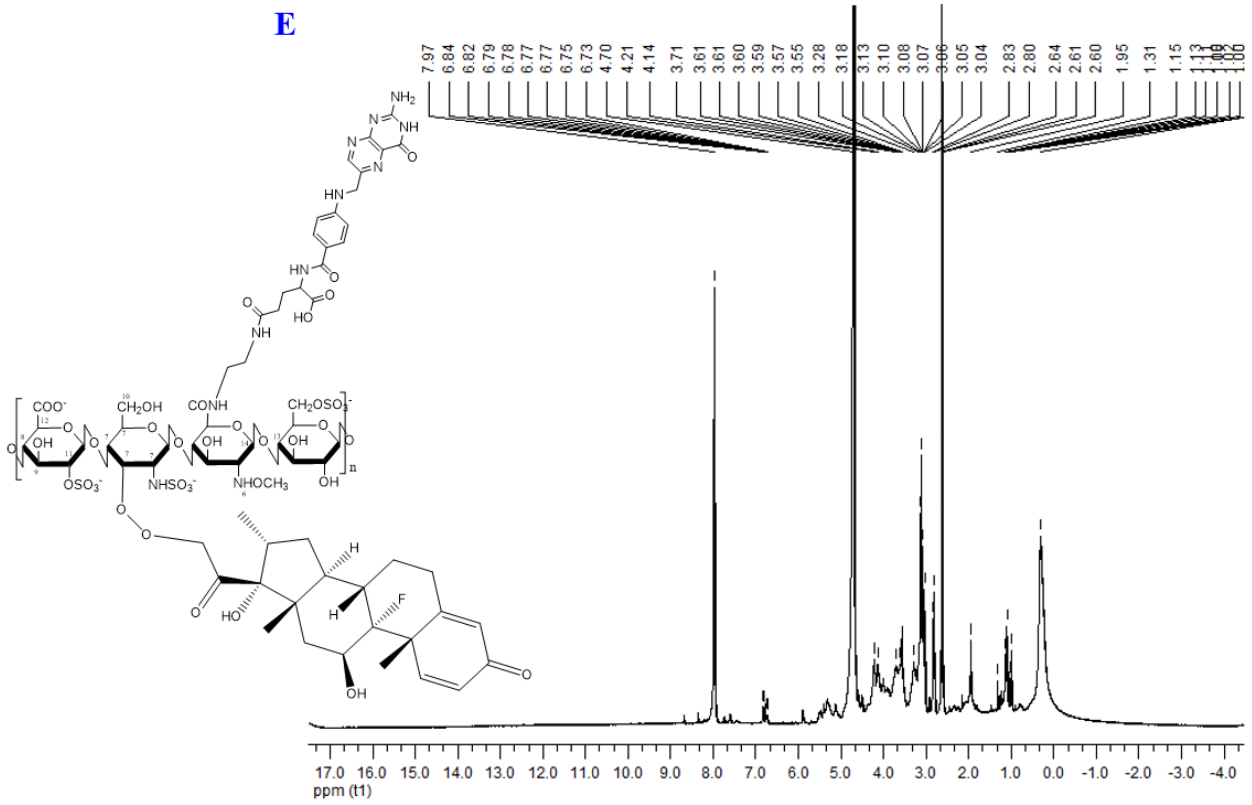

Fig. 2. ^{1}H-NMR spectra of (A) FA, (B) DEX, (C) HEP, (D) HEP-DEX, and (E) FA-HEP-DEX. FA, Folic acid; HEP, heparin; DEX, dexamethasone.

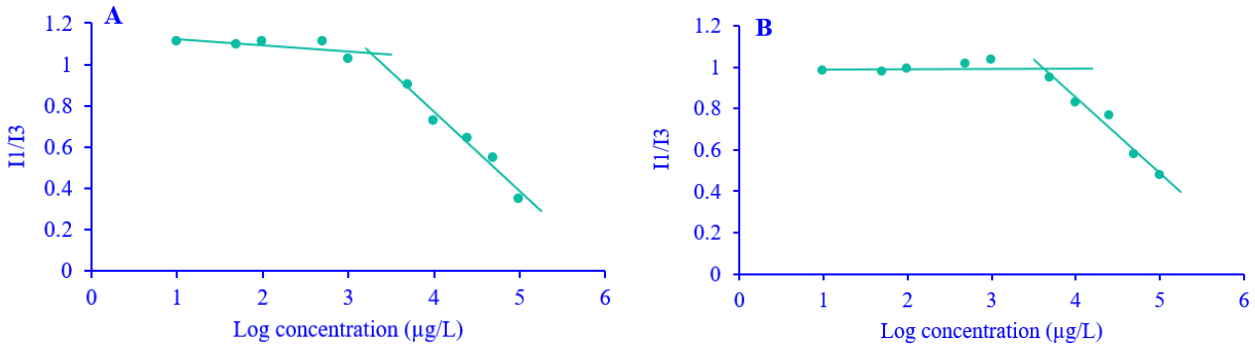

Fig. 3. Fluorescence intensity ratio variation of I_1/I_3 for pyrene emission against the logarithm of (A) HEP-DEX and (B) FA-HEP-DEX concentration. FA, Folic acid; HEP, heparin; DEX, dexamethasone.

Table 2. Physicochemical characteristics of doxorubicin-loaded micelles. Data are expressed as mean ± SD, n = 3.

Formulation	PS (nm)	ZP (mv)	EE (%)	LP (%)	MDRT (h)	PDI
$T_{25}P_2F$	155.63 ± 19.61	-25.18 ± 11.68	55.99± 20.30	18.66 ± 6.77	65.06 ± 6.88	0.0513 ± 0.0234
$T_{25}P_5F$	137.56 ± 22.40	-17.53 ± 12.18	61.53 ± 2.86	10.25 ± 0.48	51.60 ± 5.38	0.2840 ± 0.1204
$T_{45}P_2F$	117.93 ± 13.31	-36.30 ± 2.33	52.24 ± 13.86	17.41 ± 4.62	70.86 ± 6.79	0.0517 ± 0.0337
$T_{45}P_5F$	131.93 ± 13.20	-26.58 ± 8.61	71.27 ± 5.93	11.88 ± 0.98	58.05 ± 7.91	0.0621 ± 0.0693
$T_{25}P_2H$	151.73 ± 6.58	-18.61 ± 1.70	41.19 ± 0.80	13.73 ± 0.26	67.51 ± 1.24	0.2017 ± 0.1267
$T_{25}P_5H$	181.97 ± 15.72	-15.81 ± 4.86	45.85 ± 15.04	7.64 ± 2.51	62.99 ± 7.85	0.1583 ± 0.1196
$T_{45}P_2H$	145.67 ± 13.64	-20.82 ± 0.83	36.71 ± 8.16	12.26 ± 2.72	71.93 ± 7.16	0.1680 ± 0.0788
$T_{45}P_5H$	152.63 ± 24.54	-22.75 ± 2.09	49.32 ± 16.95	8.22 ± 2.83	65.78 ± 4.66	0.1127 ± 0.0354
Free drug					24.91 ± 3.45	

PS, Particle size; ZP, zeta potential; EE, entrapment efficiency; LP, loading percent; MDRT, mean drug release time; PDI, polydispersity index.

Table 3. Predicted and acquired results for the optimal formulation. Data are presented as mean ± SD, n = 3.

Parameters	Actual values	Predicted values	Error (%)
PS (nm)	112.8 ± 7.27	124.92	-9.70
ZP (mV)	-29.32 ± 5.61	-31.88	-8.03
EE (%)	58.05 ± 2.14	60.88	-4.65
MDRT (h)	71.87 ± 4.26	65.12	10.36

PS, Particle size; ZP, zeta potential; EE, entrapment efficiency; LP, loading percent; MDRT, mean drug release time

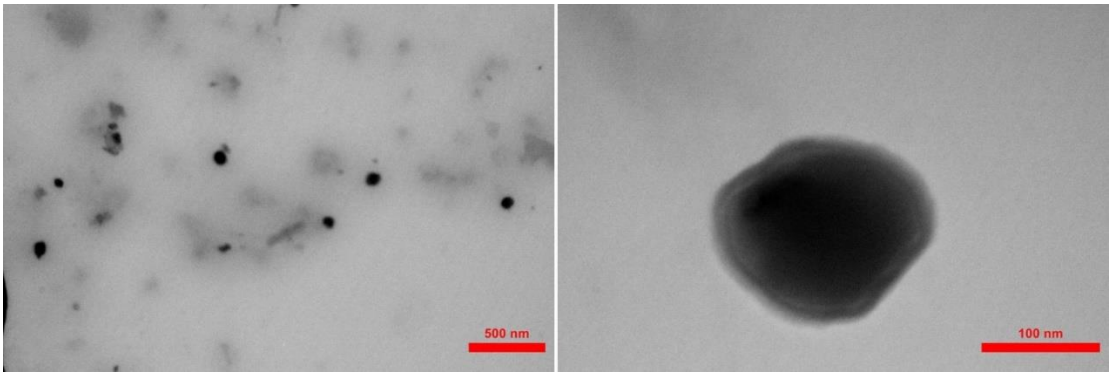

Fig. 4. Transmission electron microscopy (TEM) image of doxorubicin-loaded micelles.

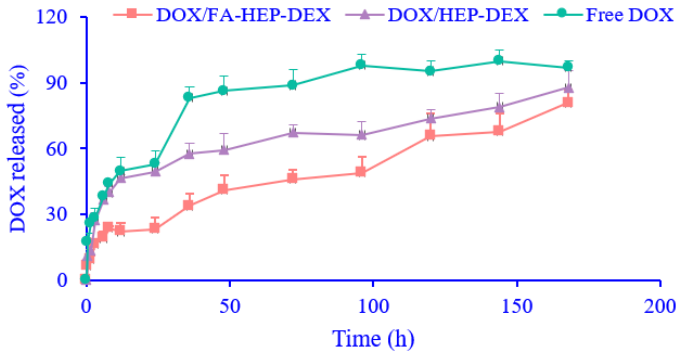

Fig. 5. DOX release profiles from the optimized formulation of DOX/FA-HEP-DEX micelles, DOX/HEP-DEX, and free DOX in PBS (pH 7.4) at 37 ℃. The data were plotted as mean ± SD, n = 3. DOX, Doxorubicin; FA, folic acid; HEP, heparin; DEX, dexamethasone.

TEM observation

The TEM image of optimized DOX/FA-HEP-DEX micelles is shown in Fig. 4 which clearly displays the uniform spherical shape of the micelles with PS around 100 nm. The smaller PS observed by TEM than that obtained by DLS was attributed to the drying process of micelles formulation for TEM observation.

Drug release from the optimized formulation

The release profiles of DOX from optimized polymeric micelles, either with or without a folate targeting ligand, as well as free DOX, are illustrated in Fig. 5.

In vitro cellular uptake

Since DOX exhibits intense red fluorescence, fluorescence microscopy enabled visualization of cellular uptake of both free DOX and DOX-encapsulated micelles.

Figures 6 and 7 show the fluorescent microscope images and mean DOX cellular uptake in K562 and HepG2 cells after 4-h incubation with free DOX, DOX/HEP-DEX micelles, or DOX/FA-HEP-DEX micelles. Cells without any treatment were used as the negative control.

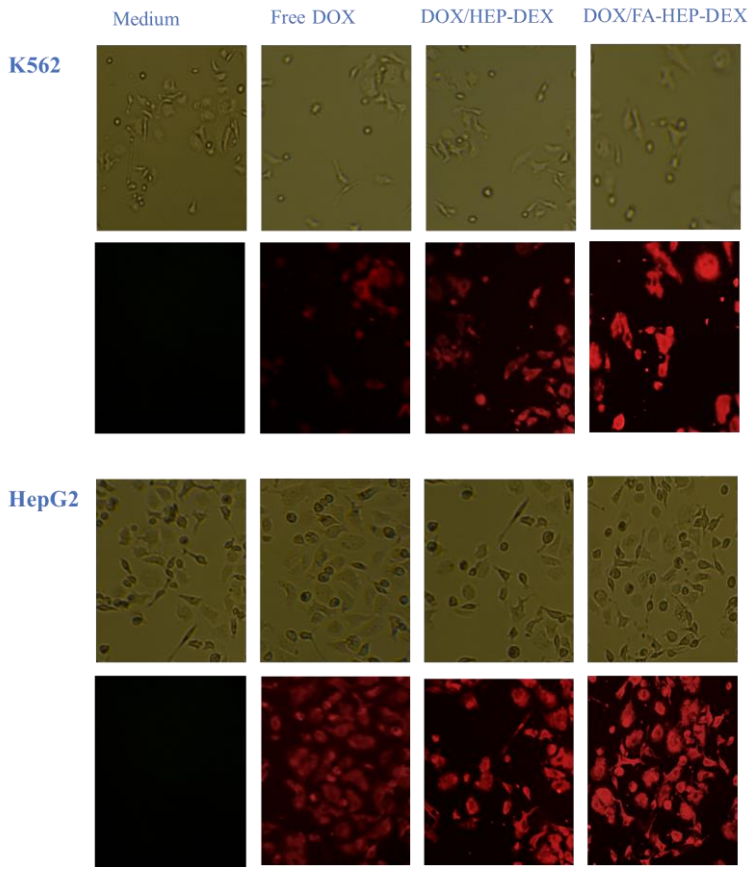

Fig. 6. Fluorescent and visible light microscopy images of K562 (rows 1 and 2) and HepG2 (rows 3 and 4) cells incubated with culture medium, free DOX, DOX/HEP-DEX, and DOX/FA-HEP-DEX micelles after 4 h incubation. DOX, Doxorubicin; FA, folic acid; HEP, heparin; DEX, dexamethasone.

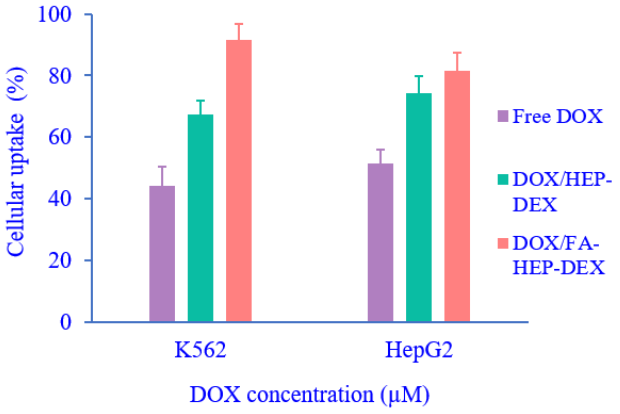

Fig. 7. The cellular uptake percentage of free DOX, DOX/HEP-DEX, and DOX/FA-HEP-DEX micelles after 4 h incubation in K562 and HepG2 cells. DOX, Doxorubicin; FA, folic acid; HEP, heparin; DEX, dexamethasone.

In vitro cell toxicity assay

The *in vitro* cytotoxicity of DOX-loaded micelles was investigated in K562 cells (which overexpress folate receptors) and HepG2 cells (which express undetectable levels of FA receptors) using an MTT assay. The cell viability after treatment with free DOX, DOX-loaded FA-HEP-DEX micelles, and DOX-loaded HEP-DEX micelles at DOX concentrations ranging from 0.01-10 μM over 48- and 72-h incubations was examined and illustrated in Fig. 8. Cells were also incubated with blank micelle formulations containing equivalent micelle quantities to the DOX-loaded formulations. The cell toxicity of the various DOX formulations (free DOX, DOX-loaded FA-HEP-DEX, and DTX-loaded HEP-DEX) was quantitatively evaluated by half-maximal inhibitory concentration (IC_{50}) values, as shown in Table 4.

In order to further evaluate the role of folate in the cellular uptake of DOX-loaded FA-HEP-DEX micelles, the cells were exposed to a constant DOX concentration of 5 μM, while free folic acid within the concentration range of 0-1000 μg/L was added to each well 30 min before the addition of DOX-loaded FA-HEP-DEX formulation. It is found that viability increased with increasing folate concentration (Fig. 9).

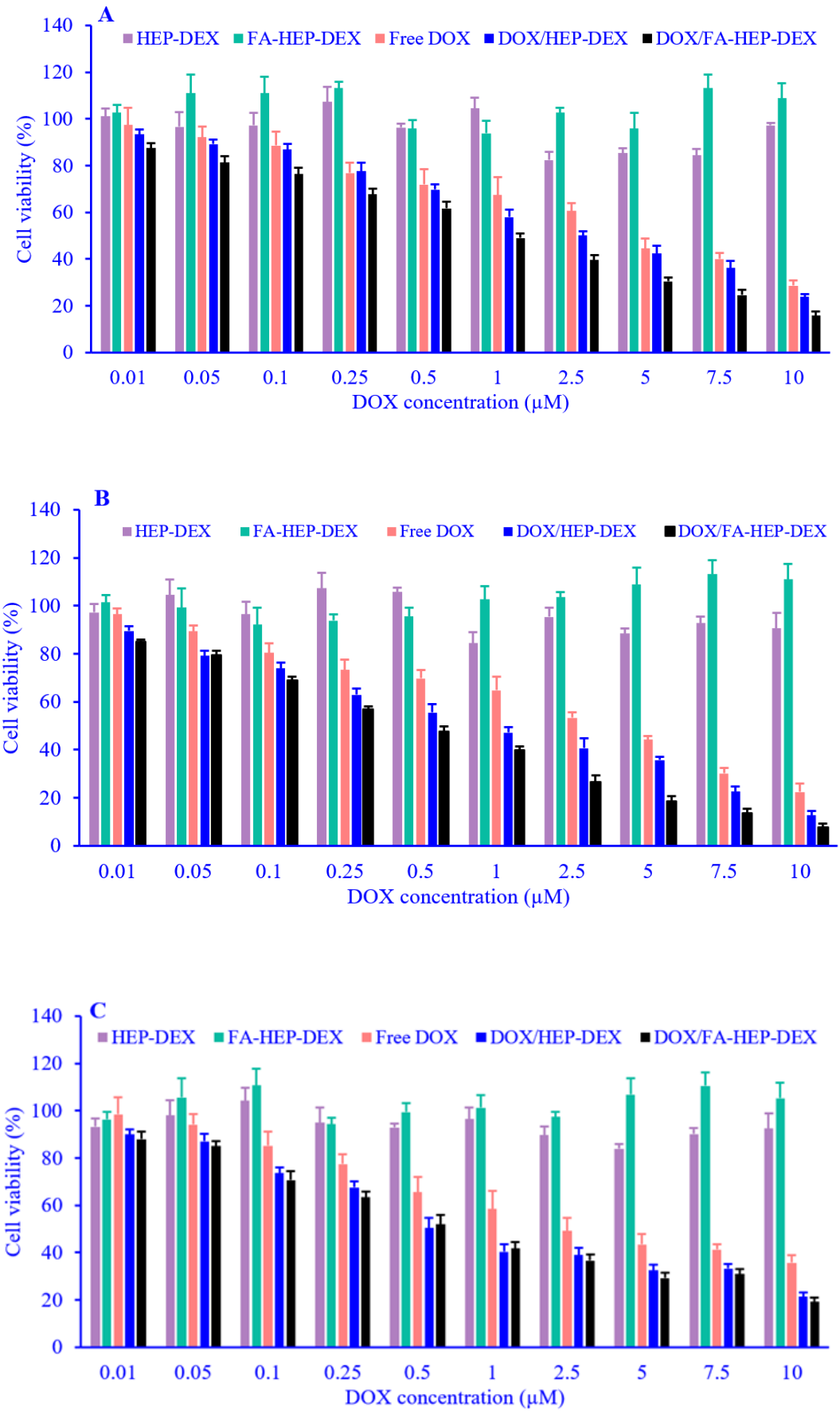
A
HEP-DEX
FA-HEP-DEX
Free DOX
DOX/HEP-DEX
DOX/FA-HEP-DEX
Cell viability (%)
0
20
40
60
80
100
120
140
0.01
0.05
0.1
0.25
0.5
1
2.5
5
7.5
10
DOX concentration (µM)
B
HEP-DEX
FA-HEP-DEX
Free DOX
DOX/HEP-DEX
DOX/FA-HEP-DEX
Cell viability (%)
0
20
40
60
80
100
120
140
0.01
0.05
0.1
0.25
0.5
1
2.5
5
7.5
10
DOX concentration (µM)
C
HEP-DEX
FA-HEP-DEX
Free DOX
DOX/HEP-DEX
DOX/FA-HEP-DEX
Cell viability (%)
0
20
40
60
80
100
120
140
0.01
0.05
0.1
0.25
0.5
1
2.5
5
7.5
10
DOX concentration (µM)

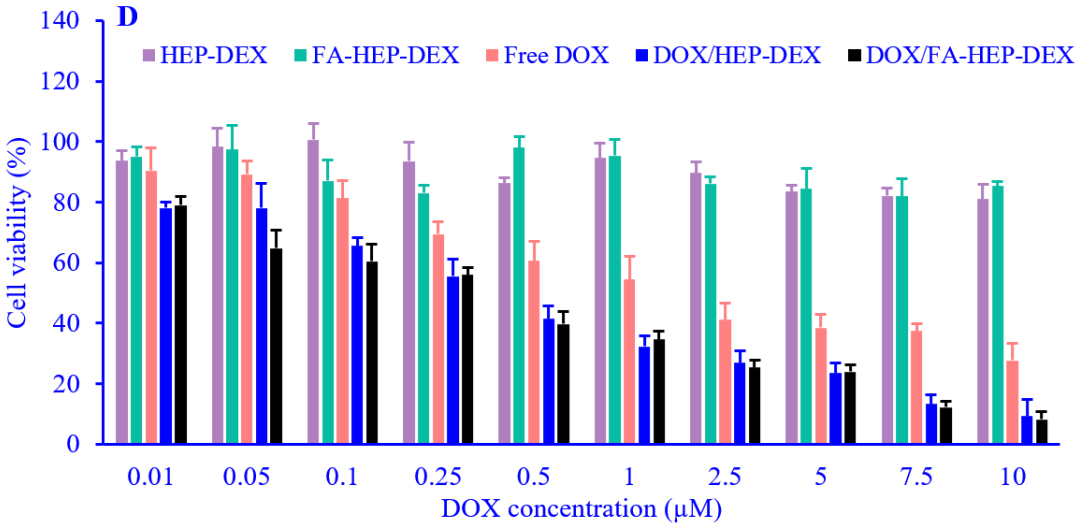

Fig. 8. *In vitro* cytotoxicity of free DOX, DOX-loaded micelles, and blank micelles evaluated against (A) K562 cells after 48 h incubation, (B) K562 cells after 72 h incubation, (C) HepG2 cells after 48 h incubation, and (D) HepG2 cells after 72 h incubation. Data are plotted as the mean ± SD, n = 3. DOX, Doxorubicin; FA, folic acid; HEP, heparin; DEX, dexamethasone.

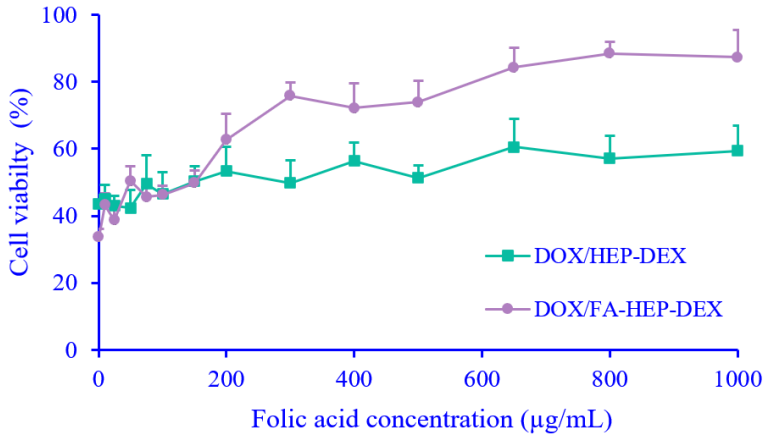

Fig. 9. Effect of free FA on the viability of K562 cells incubated with DOX/FA-HEP-DEX or DOX/HEP-DEX micelles at DOX concentration of 5 μM. Data are plotted as the mean ± SD, n = 3. DOX, Doxorubicin; FA, folic acid; HEP, heparin; DEX, dexamethasone.

Table 4. IC_{50} values of DOX from free DOX, DOX/FA-HEP-DEX and DOX/HEP-DEX micelles after 48 h and 72 h exposure to K562 and HepG2 cells. Data represent mean ± SD, n = 3. $^{**}P < 0.01$ and $^{***}P < 0.001$ represent significant differences in comparison with free DOX; $^{\#\#}P < 0.01$ versus DOX/HEP-DEX.

Formulation	K562		HepG2	
	48 h	72 h	48 h	72 h
Free DOX	3.375 ± 1.032	2.006 ± 0.832	2.735 ± 1.12	1.518 ± 0.976
DOX/HEP-DEX	2.085 ± 0.131**	0.722 ± 0.018	0.840 ± 0.06***	0.297 ± 0.082
DOX/FA-HEP-DEX	0.823 ± 0.021$^{***,\#\#}$	0.371 ± 0.007	0.716 ± 0.031***	0.234 ± 0.019

IC_{50}, Half maximal inhibitory concentration.

DISCUSSION

In the current study, heparin as the hydrophilic part of the copolymer was first modified with dexamethasone as the hydrophobic domain through esterification reactions to form amphiphilic HEP-DEX conjugates. In the next step, FA was conjugated to HEP-DEX by an amidation reaction between the carboxyl group of HEP and the free amine group of amine-terminated FA to obtain FA-HEP-DEX conjugate.

The synthesized copolymer structure was confirmed by ^{1}H-NMR. The chemical shifts at 1.92, 3.0 - 5.4, and 5.5 - 5.8 ppm which are respectively related to acetamido methyl protons, sugar ring protons, and anomeric protons, were observed in the ^{1}H-NMR spectrum of HEP (Fig. 2B), HEP-DEX (Fig. 2D), and FA-HEP-DEX (Fig. 2E).

After the chemical conjugation, the ^{1}H-NMR spectrum of the amphiphilic conjugates showed the characteristic proton peaks (Fig. 2A, D, E) of DEX at 0.71, 0.79, 1.39 ppm which can be related to the protons of the three methyls in DEX, 6.05, 6.26 and 7.39 ppm which belong to the protons of the double bonds in DEX. In the ^{1}H-NMR spectrum of FA (Fig. 2C), peaks at 1.9, 2.2, and 4.3 ppm are related to the aliphatic protons of FA. Peaks at 6.6, 7.6, and 8.6 ppm are assigned to the aromatic protons. These signals also appeared in the FA-HEP-DEX (Fig. 2E) spectrum (24,25). All these findings confirm the successful synthesis of FA-HEP-DEX conjugate.

Due to the modification of the water-soluble HEP chain with hydrophobic DEX, the synthesized amphiphilic copolymer could self-aggregate to form spherical micelles in aqueous media above the CMC. The CMC is an important parameter for evaluating dilution effects and is particularly influenced by the nature and hydrophobic domain length of the amphiphilic copolymer. Unlike conventional low molecular weight surfactants, polymeric micelles have the advantage of possessing very low CMC values. Lower CMC values indicate greater thermodynamic stability of the micelles, which helps maintain their structural integrity during dilution by body fluids. In this study, we determined the CMC of amphiphilic copolymers (HEP-DEX and FA-HEP-DEX) using a fluorescent dye solubilization approach with pyrene as the hydrophobic probe. The intensity ratio (I_1/I_3) of the first (336 nm) and the third (390 nm) vibronic peaks of pyrene was used as an indicator to estimate the polarity of the pyrene microenvironment. The relative intensity ratio of the first and third vibronic bands in pyrene's emission spectrum can indicate the polarity of the pyrene environment. This ratio is used to determine the CMC because pyrene experiences a different microenvironment when micelles form. In a polar environment (*e.g.* water), the I_1 band intensity is higher than the I_3 band. The spectrum is dominated by the I_1 band. In a nonpolar, hydrophobic environment (*e.g.* inside the micelle core), the I_3 band intensity increases over the I_1 band. As amphiphilic polymers form micelles above the CMC, pyrene molecules incorporated in the nonpolar core show a decrease in the I_1/I_3 ratio. Plotting the I_1/I_3 ratio versus polymer concentration shows an abrupt decrease at the CMC due to pyrene partitioning into the micelle cores. Therefore, the I_1/I_3 ratio reflects changes in pyrene's local environment and can indicate micelle formation (26).

Figure 3 shows the fluorescence intensity ratios (I_1/I_3) against the logarithm of concentrations of two polymers. As illustrated in Fig. 3A and B, at lower polymer concentrations, the intensity ratios of I_1/I_3 were observed in constant values. With a further increase in polymer concentration, due to micelles formation, the pyrene molecules are preferably partitioned into the less polar hydrophobic micelles core, consequently resulting in an increase of the third peak intensity as well as a decrease in I_1/I_3 values.

The CMCs were calculated from the intersection of the two straight lines in the curve of intensity ratios of I_1/I_3 against the logarithm of FA-HEP-DEX or HEP-DEX concentrations. The CMC values of FA-HEP-DEX and HEP-DEX were 4.206 and 1.806 µg/mL, respectively. The CMC values for targeted micelles found in the current study are much lower than those of some traditional low-molecular-weight surfactants (10^{-1} - 10^{-4} M) and other HEP-based or folate-conjugated polymeric micelles reported in previous studies (26-29). Low CMC values are desired to avoid the micelle's dissociation upon dilution in blood circulation following intravenous injection. The CMC of FA-HEP-DEX was slightly higher

than that of HEP-DEX indicating that the folate conjugation has little bearing on the micelle self-aggregation behavior.

However, the HEP-DEX still formed stable self-assembled nanoparticles at low concentrations and the CMC values of these copolymers are good enough to maintain micellar stability upon intravenous administration.

In this study, DOX was co-loaded with DEX using folate-targeted micelles for combination drug delivery to the leukemic cells. Due to lipophilic properties, DOX was mainly incorporated into the hydrophobic core of the micelle. Several parameters such as drug physicochemical properties, preparation method, hydrophobic interactions between drug and micelle core, and P/D can affect EE. As a result, the EE of DOX in the micelles was in the range of 36% to 71% and the LP values were found to be 8% to 18% (Table 2).

According to the results, the solvent type initially used in the dialysis process was the most effective factor on EE, *i.e.* EE increased significantly by switching the solvent from THF to DMF ($P < 0.01$). The higher drug entrapment in micelles prepared by DMF can be attributed to the polarity index and greater miscibility of DMF with water. This greater miscibility resulted in the rapid removal of DMF from the dialysis bag and copolymer precipitation, which increased drug entrapment in the micelles (26).

EE of DOX in the micelles also increased significantly as P/D increased during micelle preparation ($P < 0.05$). This finding could be explained by the fact that an increase in the P/D ratio provides more micellar structure and entrapment sites, consequently improving drug solubilization and incorporation efficiency into the hydrophobic micelle core. The increased P/D ratio enables stronger hydrophobic interactions between DOX and the DEX segments compared to DOX interactions with the solvent or other DOX molecules. Under these conditions, DOX preferentially incorporates into the organized micelle core rather than randomly precipitating out, resulting in higher DOX EE. This finding is in accordance with previous studies such as those conducted by Yokoyama *et. al.* (27) who explained the effects of copolymer concentration and solvent type used in the dialysis procedure on drug EE. In addition, Gill *et al.* reported that the EE of PTX in PEG-DSPE micelles was enhanced by increasing the polymer concentration (29). In contrast, Huang *et al.* reported that the EE of DOX increased *via* increasing the drug-to-polymer ratio up to 10:5. Above this ratio increasing in drug concentration showed a reverse effect on EE (30).

PS is a critical nanoparticle feature influencing blood circulation time, therapeutic efficacy, cellular uptake, and tumor accumulation through the enhanced permeability and retention (EPR) effect. Studies demonstrate nanoparticles with diameters under 200 nm can permeate cancerous tissues while evading reticuloendothelial system clearance (31,32).

In the current study, the PS of the designed DOX-loaded polymeric micelles was measured by dynamic light scattering. The PS of the polymeric micelles, as shown in Table 2, ranging from 117 to 181 nm, ideal dimensions for passive tumor targeting *via* the EPR effect. PDI values between 0.05 and 0.28, under the 0.3 threshold, verified the micelles formed a homogeneous system without extensive aggregation. This uniformity of nano-sized micelles is advantageous for injectable drug delivery applications.

Because micelles were prepared by dialysis methods, an organic solvent type that was initially used in the dialysis process to dissolve copolymer should be water-miscible. Therefore, it could be anticipated that solvent-polymer or solvent-water miscibility could affect micelle formation (31,32).

According to the results, the micelles prepared with THF during dialysis showed larger PS compared to those prepared with DMF ($P < 0.01$). This indicates the solvent used to dissolve the copolymer significantly impacts the resulting micelle size and distribution.

The water miscibility of the solvents depends on their dielectric constant and polarity. DMF has a higher polarity index (~6.4) than THF (~4), conferring greater water miscibility. The enhanced miscibility of DMF led to its rapid removal from the dialysis bag and copolymer precipitation. Faster precipitation produces smaller PS. In our previous work, we investigated the effects of different solvents initially used in dialysis,

DMSO *vs* DMF, on micelle size (28). As expected, larger particles were achieved when DMSO was used as an organic solvent during dialysis. This can be attributed to the higher polarity index of DMSO compared to DMF resulting in more water miscibility of DMSO than DMF. All these findings can prove the role of dialysis solvent on the PS of the micelles as discussed in some previous studies (27,33). For instance, in the study conducted by Kim and coworkers, the indomethacin-loaded micelles prepared using DMF exhibited smaller sizes compared to those prepared using THF as a dialysis solvent (31).

Another factor that influences the PS of the micelles is the temperature during the dialysis process. As shown in Table 2, the PS of the micelles decreased as the dialysis temperature increased. PS of micellar systems can be impacted by structural transitions between vesicles and micelles, typically triggered by altering environmental factors such as pH, temperature, light, and CO_2 concentration. Parikh *et al*. previously reported that increasing the temperature of a cationic gemini surfactant solution induced micelle-to-vesicle transitions, enlarging PS and distribution (34). However, in this study, no evident micelle-to-vesicle transitions or aggregate fusion occurred with rising temperature, as confirmed by the PDI results. As shown in Table 2, PDI values decreased as temperature increased, indicating the micellar dispersion remained homogeneous and mono-modal even at higher temperatures.

The ZP signifies the potential stability of a colloidal system. Dispersions with large negative or positive ZP tend to have better resistance to aggregation. As shown in Table 2, the DOX-loaded polymeric micelles developed in the current study exhibited strongly negative ZP from -15.8 to -36.3 mV, confirming formulation stability through electrostatic repulsion hindering adsorption of anionic proteins after systemic delivery (35).

The results show solvent type and temperature influence ZP ($P < 0.05$). Micelle absolute ZP significantly increased ($P < 0.05$) at higher temperatures or when switching the dialysis solvent from THF to DMF. As mentioned, smaller particles were attained using DMF or higher temperatures during dialysis, which increased the surface charge density of the micelles. These findings align with Varshosaz *et al*. showing that PS reduction causes greater micelle surface charge density (28).

A controlled drug release profile is an essential requirement for an optimal drug carrier to prevent premature release before reaching the intended site, particularly crucial for anticancer drugs.

Table 2 presents the MDRTs of DOX from the various micellar formulations over 168 h at 37 °C, demonstrating their controlled release capabilities.

In contrast to the rapid release of free DOX from the cellulose membrane, the release of DOX from the drug-loaded micelles exhibited a markedly slower and sustained release pattern. The initial burst release observed within the first 8 h can be attributed to the release of the drug located near the micelle surface. Following this initial phase, the sustained release over subsequent hours reflected the diffusion of the drug from the core of the micelles. The drug release rate also decreases with the attachment of folic acid to the surface of the micelles. The observed decrease in the rate and manner of drug release when FA is conjugated on the surface of the micelles can be interpreted through the following mechanisms:

Folic acid conjugation may enhance the structural integrity of the micelles due to increased molecular interactions, such as hydrogen bonding or π-π stacking between FA molecules and other micelle components. This can lead to a more compact and stable micellar structure, reducing the rate of drug diffusion from the core. The conjugation may stabilize the micelle assembly, making it less prone to disintegration under physiological conditions, thereby slowing drug release. The conjugation of FA, a hydrophilic molecule, can increase the hydrophilicity of the micelle surface. This hydrophilic "shell" might act as a barrier, impeding the diffusion of the drug from the hydrophobic core to the surrounding aqueous environment. FA can interact with the drug directly, either through hydrogen bonding or other non-covalent interactions, leading to drug retention within the micelle. If the conjugated FA modifies the chemical environment of the micelle surface, it might reduce the propensity of the drug to partition out of the micelle. FA conjugation may shift the drug release

mechanism from simple diffusion to a more controlled, stimulus-responsive release. For example, the micelles may require specific triggers (*e.g.* acidic pH or enzymatic degradation) to break down the FA layer and release the drug.

As illustrated in Fig. 5, approximately 60-65% of the loaded drug was released in a sustained manner beyond the initial 10-h period of the release test. This finding is significant as it suggests that the formulation and delivery system used in the study is capable of providing a sustained release of the drug, which can have potential benefits in various applications such as drug delivery systems for targeted therapies or long-term treatment regimens.

Among the studied variables, the P/D ratio was the most effective factor in the rate of drug release from the micelles ($P < 0.01$). Increasing the P/D significantly lowered the MDRT, explainable by the declining drug content within the micelles. As shown in Table 2, the drug content decreased as the P/D ratio increased, indicating a greater amount of polymer relative to the quantity of drug loaded in the micelles. At higher polymer ratios, less encapsulated drug leads to faster release rates (lower MDRT value). Based on these results, it was concluded that the rate of drug release appears to depend on the amount of drug encapsulated inside the micelle core. This finding aligns with Xiao *et al.* who reported increased release of indomethacin nanospheres with reduced loading, attributed to enhanced drug-carrier hydrophobic interactions.

The slower release of hydrophobic micelle-encapsulated drugs is commonly observed at higher loadings where more drug resides in the hydrophobic core. For example, Jeong et al. showed hydrophobic drugs adriamycin and clonazepam displayed slower release from PEG-PBLG micelles at higher loadings (36,37). Similarly, lidocaine-PEG-PLGA micelles exhibited accelerated release kinetics at lower drug loading. The decreased release rate likely arises from drug crystallinity and stronger hydrophobic interactions between the micelle core and drug when the content is higher. At higher drug loadings, multiple factors arising from the high local drug concentration, thermodynamics, molecular interactions, and the core microenvironment in micelles can promote drug crystallization and aggregation (38).

The micelles prepared using THF exhibited higher MDRT values than those prepared using DMF ($P < 0.05$). This could be attributed to the larger particle size of micelles formed using THF as the initial solvent, which in turn decreases the drug release rate. As mentioned earlier, PS is an important feature affecting nanoparticle behavior such as drug release kinetics. Based on Fick's law, a decrease in PS leads to an increase in drug release rate due to an increasing surface area to volume ratio and decreasing diffusion path length. The effect of reduced PS on enhancing drug release from nanocarriers has been demonstrated in previous studies.

Realizing maximal therapeutic efficacy necessitates effective intracellular delivery of drug-loaded nanoparticles (39). Although nonspecific accumulation of nanoparticles in tumors *via* the EPR effect may occur, this does not necessarily translate to antitumor activity without efficient cellular internalization to enable engagement of the cytotoxic drug with its intracellular target. Since DOX exhibits intense red fluorescence, fluorescence microscopy enabled visualization of cellular uptake of both free DOX and DOX-encapsulated micelles.

K562 cells which over-expressed folate receptors were used as folate receptor positive cells and HepG2 cells which express folate receptors at undetectable levels were used as folate receptor negative cells. Cells without any treatment were also used as the negative control. Figure 6 shows the fluorescence image of the cells incubated with free DOX, DOX/HEP-DEX and DOX/FA-HEP-DEX after 4 h.

Figure 6 shows no red fluorescence in untreated cells, while clear DOX auto-fluorescence appears in cells treated with free DOX, DOX/HEP-DEX micelles, and DOX/FA-HEP-DEX micelles. This indicates successful cellular internalization of DOX. As shown in Figure 6, K562 cells treated with DOX/FA-HEP-DEX micelles exhibited stronger red fluorescence intensity compared to those treated with DOX/HEP-DEX micelles or free DOX. This indicates the FA ligand enhanced cellular uptake of DOX/FA-HEP-DEX in K562 cells, which overexpress folate receptors. In contrast, no significant difference was observed between fluorescence intensities

in HepG2 cells treated with DOX/FA-HEP-DEX versus DOX/HEP-DEX.

Fluorometric measurement of cellular uptake supported these findings. Figure 7 shows the mean DOX cellular uptake in K562 and HepG2 cells after 4 h incubation with free DOX, DOX/HEP-DEX micelles, or DOX/FA-HEP-DEX micelles. Cells treated with DOX-loaded micelles (DOX/HEP-DEX or DOX/FA-HEP-DEX) exhibited higher mean cellular uptake than cells incubated with free DOX, associated with greater DOX release from the internalized micelles. However, folate receptor-positive K562 cells showed very weak internalization when treated with free DOX or DOX/HEP-DEX micelles, while DOX/FA-HEP-DEX micelles produced higher cellular uptake in these cells.

In contrast to K562 cells, no significant difference in cellular uptake was observed between HepG2 cells treated with DOX-loaded FA-HEP-DEX versus plain HEP-DEX micelles. This finding suggests that the enhanced uptake of DOX/FA-HEP-DEX micelles by K562 cells can be attributed specifically to folate receptor-mediated endocytosis, enabled by the FA ligand targeting this receptor which is highly expressed on K562 cells but not HepG2 cells. The lack of difference between the two micelle formulations in HepG2 cells, which have minimal folate receptor expression, further supports the notion that the FA-targeting ligand conferred selective and receptor-mediated internalization.

In our previous works, a folate-targeted alpha-tocopherol conjugate containing HEP demonstrated greater cell internalization in folate overexpressing 4T1 cells compared to HepG2 cells. Docetaxel-loaded micelles conjugated with folate were also taken up to a greater extent by MCF-7 cells, which overexpress folate receptors, than by HepG2 cells. This increased micellar cellular uptake is likely due to the high-affinity binding of the folate conjugate to folate receptors and subsequent folate receptor-mediated endocytosis (20,21). These findings align with previous studies showing enhanced cellular uptake of folate-targeted carriers in cells overexpressing folate receptors. For instance, Kumar *et al.* showed folate-conjugated liposomes exhibited 100-fold greater uptake by KB cells (which overexpress folate receptors) compared to non-targeted liposomes (40). In another study, Wang *et al.* demonstrated increased cellular internalization of folate-linked micelles by MCF-7 and HeLa cells through receptor-mediated endocytosis (39).

Overall, the intracellular tracking studies demonstrate efficient delivery of the DOX payload mediated by the FA-targeted micelles specifically to FR-overexpressing tumor cells. Moving forward, it will be critical to demonstrate that this enhanced, receptor-mediated uptake translates to superior antitumor activity against FA receptor-positive versus FA receptor-negative cells in cytotoxicity assays, which are discussed in the next section.

As shown in Fig. 8, empty HEP-DEX and FA-HEP-DEX (blank micelles) did not demonstrate toxicity against any of the tested cell types, even at high micellar component concentrations. This indicates that the HEP-modified polymeric micelles have adequate biocompatibility and safety for drug delivery applications. However, all DOX-containing formulations exhibited drug concentration-dependent toxicity in both tested cell lines after 48 and 72 h. Furthermore, cell viability was lower after 72 h compared to 48 h (Fig. 8A-D). Both targeted and non-targeted DOX-loaded micelles exhibited greater cell toxicity against cancer cells compared to free DOX. The cytotoxicity of DOX delivered by DOX/FA-HEP-DEX against K562 cells was also higher than DOX/HEP-DEX (Fig. 8A and B). However, the cytotoxicity of DOX/FA-HEP-DEX and DOX/HEP-DEX against HepG2 cells was nearly identical (Fig. 8C and D).

The IC_{50} value for DOX/FA-HEP-DEX against K562 cells was significantly lower than that of free DOX and DOX/HEP-DEX micelles. Furthermore, no significant difference was seen between IC_{50} values of DOX/FA-HEP-DEX and DOX/HEP-DEX against HepG2 cells. The high cell toxicity of DOX/FA-HEP-DEX is likely due to folate receptor binding by the FA ligand, resulting in increased micellar cellular uptake *via* folate receptor-mediated endocytosis.

However, at higher concentrations, the toxicity of DOX/FA-HEP-DEX and DOX/HEP-DEX did not significantly differ, indicating a reduced FA targeting effect

potentially due to folate receptor saturation. This was further confirmed through a competitive inhibition study using free FA. The affinity of DOX/FA-HEP-DEX and non-targeted DOX/HEP-DEX micelles to folate receptor-overexpressing K562 cells was indirectly evaluated by examining cell viability. Generally, reduced cytotoxicity (increased cell viability) of DOX-loaded nanoparticles corresponds to decreased nanoparticle cellular uptake. To verify folate receptor-mediated uptake of DOX/FA-HEP-DEX, competition between the folate-targeted micelles and free FA for uptake by K562 cells was tested (Fig. 9). In folate receptor-overexpressing K562 cells treated with DOX/FA-HEP-DEX, cell viability increased with increasing concentrations of free FA in the medium and reached a plateau state at a certain level of free FA. This suggests the presence of free FA reduced DOX/FA-HEP-DEX cellular uptake by saturating folate receptors (Fig.9). These results indicate DOX/FA-HEP-DEX micelles enter K562 cells *via* folate receptors, analogous to free folic acid.

Control experiments were performed with non-targeted DOX/HEP-DEX micelles. As expected, DOX/HEP-DEX treated cells showed no distinct change in cell viability with added free FA, indicating DOX/HEP-DEX micelles have negligible ability to compete with FA for cell entry. Overall, the results demonstrated that the presence of FA on the micelle surface plays a major role in cellular uptake and toxicity against FA-overexpressing cells. The cytotoxicity results demonstrated dose- and time-dependent decreases in cancer cell viability when treated with both free and micelle-encapsulated drug formulations. Higher drug concentrations and longer incubation times generally resulted in enhanced antiproliferative effects. Furthermore, the micelles conjugated with folic acid to enable active targeting exhibited greater chemotherapeutic efficacy compared to non-targeted micelles and free drugs across most of the conditions tested. This provides evidence that the folate-mediated targeting strategy improved the delivery of the chemotherapeutic payload to folate receptor-overexpressing cancer cells, consequently enhancing antineoplastic activity.

Previous studies have also reported enhanced tumor cell toxicity by incorporating FA into micelle surfaces (41,42). For example, folate-targeted tamoxifen-loaded poly-caprolactone micelles exhibited higher toxicity against MCF-7 cells compared to non-targeted micelles, attributed to receptor-mediated endocytosis (43).

CONCLUSION

DOX-loaded folate-targeted micelles composed of biocompatible polymer were synthesized and prepared using the dialysis method. Based on the analysis, PS and EE were mainly affected by solvent type while P/D and temperature were the most effective parameters on MDRT and ZP, respectively. The release profiles of DOX from polymeric micelles demonstrated an initial rapid-release phase reflecting the drug loaded near the micelle surface or core-shell interface. Once this interfacial drug was depleted, the release profile transitioned to a more gradual, sustained release pattern over subsequent hours, consistent with the diffusion of DOX from the stable micelle core. These results reveal the ability of polymeric micelles to provide sustained release of potent hydrophobic chemotherapeutics. The study found that folate-targeted micelles increased the anticancer effect of DOX in human erythroleukemic cancer cells compared to free DOX and non-targeted micelles. This was due to FA receptor-mediated endocytosis, which allowed the micelles to be taken up by the cancer cells more efficiently. The study's findings provide important insights into the use of folate-targeted biocompatible polymeric micelles for targeted delivery of anticancer drugs. This approach has the potential to improve drug efficacy and reduce off-target effects by targeting cancer cells more effectively.

Acknowledgments

This study was financially supported by the Vice Chancellor of Research of Isfahan University of Medical Sciences, I.R. Iran through Grant No. 189136.

Conflict of interest statements

The authors declared no conflict of interest in this work.

Authors' contributions

J. Emami contributed to the concept, study design, definition of intellectual content, data analysis, manuscript editing and review; M. Kazemi contributed to literature search, experimental studies, data acquisition, statistical analysis, and manuscript preparation; and M. Mirian contributed to cell culture study design. All authors read and approved the finalized article.

REFERENCES

1. Miranda-Filho A, Piñeros M, Ferlay J, Soerjomataram I, Monnereau A, Bray F. Epidemiological patterns of leukaemia in 184 countries: A population-based study. Lancet Haematol. 2018;5(1):e14-e24. DOI: 10.1016/s2352-3026(17)30232-6.
2. Torre LA, Siegel RL, Ward EM, Jemal A. Global cancer incidence and mortality rates and trends-an update. Cancer Epidemiol Biomarkers Prev. 2016;25(1):16-27. DOI: 10.1158/1055-9965.EPI-15-0578.
3. Taylor J, Xiao W, Abdel-Wahab O. Diagnosis and classification of hematologic malignancies on the basis of genetics. Blood. 2017;130(4):410-423. DOI: 10.1182/blood-2017-02-734541.
4. Rezazadeh M, Akbari V, Amuaghae E, Emami J. Preparation and characterization of an injectable thermosensitive hydrogel for simultaneous delivery of paclitaxel and doxorubicin. Res Pharm Sci. 2018;13(3):181-191. DOI: 10.4103/1735-5362.228918.
5. Jabbour E, Cortes JE, Ghanem H, O'Brien S, Kantarjian HM. Targeted therapy in chronic myeloid leukemia. Expert Rev Anticancer Ther. 2008;8(1):99-110. DOI: 10.1586/14737140.8.1.99.
6. Sercombe L, Veerati T, Moheimani F, Wu SY, Sood AK, Hua S. Advances and challenges of liposome assisted drug delivery. Front Pharmacol. 2015;6:286,1-13. DOI: 10.3389/fphar.2015.00286.
7. Coukell AJ, Brogden RN. Liposomal amphotericin B. Therapeutic use in the management of fungal infections and visceral leishmaniasis. Drugs. 1998;55:585-612. DOI: 10.2165/00003495-199855040-00008.
8. Allen TM. Liposomal drug formulations. Rationale for development and what we can expect for the future. Drugs. 1998;56(5):747-756. DOI: 10.2165/00003495-199856050-00001.
9. Akbarzadeh A, Rezaei-Sadabady R, Davaran S, Joo SW, Zarghami N, Hanifehpour Y, *et al*. Liposome: classification, preparation, and applications. Nanoscale Res Lett. 2013;8(1):102,1-9. DOI: 10.1186/1556-276X-8-102.
10. Bozzuto G, Molinari A. Liposomes as nanomedical devices. Int J Nanomed. 2015:975-999. DOI: 10.2147/IJN.S68861.
11. Flühmann B, Ntai I, Borchard G, Simoens S, Mühlebach S. Nanomedicines: the magic bullets reaching their target? Eur J Pharm Sci. 2019;128: 73-80. DOI: 10.1016/j.ejps.2018.11.019.
12. Zhao W, Zhuang S, Qi XR. Comparative study of the *in vitro* and *in vivo* characteristics of cationic and neutral liposomes. Int J Nanomed. 2011;6:3087-3098. DOI: 10.2147/IJN.S25399.
13. Bulbake U, Doppalapudi S, Kommineni N, Khan W. Liposomal formulations in clinical use: an updated review. Pharmaceutics. 2017;9(2):12,1-13. DOI: 10.3390/pharmaceutics9020012.
14. Akimoto H, Bruno NA, Slate DL, Billingham ME, Torti SV, Torti FM. Effect of verapamil on doxorubicin cardiotoxicity: altered muscle gene expression in cultured neonatal rat cardiomyocytes. Cancer Res. 1993;53(19):4658-4664. PMID: 8402643.
15. Ito H, Miller SC, Billingham ME, Akimoto H, Torti SV, Wade R, *et al*. Doxorubicin selectively inhibits muscle gene expression in cardiac muscle cells *in vivo* and *in vitro*. Proc Natl Acad Sci USA. 1990;87(11):4275-4279. DOI: 10.1073/pnas.87.11.4275.
16. Inaba H, Pui CH. Glucocorticoid use in acute lymphoblastic leukaemia. Lancet Oncol. 2010;11(11):1096-1106. DOI: 10.1016/S1470-2045(10)70114-5.
17. Krishnan V, Xu X, Barwe SP, Yang X, Czymmek K, Waldman SA, *et al*. Dexamethasone-loaded block copolymer nanoparticles induce leukemia cell death and enhance therapeutic efficacy: A novel application in pediatric nanomedicine. Mol Pharm. 2013;10(6):2199-2210. DOI: 10.1021/mp300350e.
18. Salimi A, Sharif Makhmal Zadeh B, Kazemi M. Preparation and optimization of polymeric micelles as an oral drug delivery system for deferoxamine mesylate: *in vitro* and *ex vivo* studies. Res Pharm Sci. 2019;14(4):293-307. DOI: 10.4103/1735-5362.263554.
19. Kazemi M, Emami J, Hasanzadeh F, Minaiyan M, Mirian M, Lavasanifar A. Development of a RP-HPLC method for analysis of docetaxel in tumor-bearing mice plasma and tissues following injection of docetaxel-loaded pH responsive targeting polymeric micelles. Res Pharm Sci. 2020;15(1):1-13. DOI: 10.4103/1735-5362.278710.
20. Kazemi M, Emami J, Hasanzadeh F, Minaiyan M, Mirian M, Lavasanifar A, *et al*. *In vitro* and *in vivo* evaluation of novel DTX-loaded multifunctional heparin-based polymeric micelles targeting folate receptors and endosomes. Recent Pat Anticancer Drug Discov. 2020;15(4):341-359. DOI: 10.2174/1574892815666201006124604.
21. Kazemi M, Emami J, Hasanzadeh F, Minaiyan M, Mirian M, Lavasanifar A. Pegylated multifunctional pH-responsive targeted polymeric micelles for ovarian cancer therapy: synthesis, characterization and pharmacokinetic study. Int J Polym Mater. 2021;70(14):1012-1026. DOI: 10.1080/00914037.2020.1776282.

22. Li L, Huh KM, Lee YK, Kim SY. Design of a multifunctional heparin-based nanoparticle system for anticancer drug delivery. Macromol Res. 2010;18:153-161. DOI: 10.1007/s13233-009-0134-8.
23. Emami J, Kazemi M, Salehi A. *In vitro* and *in vivo* evaluation of two hydroxychloroquine tablet formulations: HPLC assay development. J Chromatogr Sci. 2021;59(1):71-78. DOI: 10.1093/chromsci/bmaa079.
24. Midelfart A, Dybdahl A, Müller N, Sitter B, Gribbestad IS, Krane J. Dexamethasone and dexamethasone phosphate detected by 1H and 19F NMR spectroscopy in the aqueous humour. Exp Eye Res. 1998;66(3):327-337. DOI: 10.1006/exer.1997.0429.
25. Kim D, Lee ES, Oh KT, Gao ZG, Bae YH. Doxorubicin-loaded polymeric micelle overcomes multidrug resistance of cancer by double-targeting folate receptor and early endosomal pH. Small. 2008;4(11):2043-2050. DOI: 10.1002/smll.200701275.
26. Yang X, Cai X, Yu A, Xi Y, Zhai G. Redox-sensitive self-assembled nanoparticles based on alpha-tocopherol succinate-modified heparin for intracellular delivery of paclitaxel. J Colloid Interface Sci. 2017;496:311-326. DOI: 10.1016/j.jcis.2017.02.033.
27. Yokoyama M, Satoh A, Sakurai Y, Okano T, Matsumura Y, Kakizoe T, *et al*. Incorporation of water-insoluble anticancer drug into polymeric micelles and control of their particle size. J Control Release. 1998;55(2-3):219-229. DOI: 10.1016/s0168-3659(98)00054-6.
28. Taymouri S, Varshosaz J, Hassanzadeh F, Haghjooy Javanmard S, Dana N. Optimisation of processing variables effective on self-assembly of folate targeted Synpronic-based micelles for docetaxel delivery in melanoma cells. IET Nanobiotechnol. 2015;9(5): 306-313. DOI: 10.1049/iet-nbt.2014.0076.
29. Gill KK, Nazzal S, Kaddoumi A. Paclitaxel loaded PEG(5000)-DSPE micelles as pulmonary delivery platform: formulation characterization, tissue distribution, plasma pharmacokinetics, and toxicological evaluation. Eur J Pharm Biopharm. 2011;79(2):276-284. DOI: 10.1016/j.ejpb.2011.04.017.
30. Huang X, Liao W, Zhang G, Kang S, Zhang CY. pH-sensitive micelles self-assembled from polymer brush (PAE-g-cholesterol)-b-PEG-b-(PAE-g-cholesterol) for anticancer drug delivery and controlled release. Int J Nanomedicine. 2017;12:2215-2226. DOI: 10.2147/IJN.S130037.
31. Kim SY, Shin IG, Lee YM, Cho CS, Sung YK. Methoxy poly (ethylene glycol) and ϵ-caprolactone amphiphilic block copolymeric micelle containing indomethacin.: II. Micelle formation and drug release behaviours. J Control Release. 1998;51(1):13-22. DOI: 10.1016/s0168-3659(97)00124-7.
32. Shin IG, Kim SY, Lee YM, Cho CS, Sung YK. Methoxy poly (ethylene glycol)/ϵ-caprolactone amphiphilic block copolymeric micelle containing indomethacin.: I. Preparation and characterization. J Control Release. 1998;51(1):1-11. DOI: 10.1016/s0168-3659(97)00164-8.
33. La SB, Okano T, Kataoka K. Preparation and characterization of the micelle-forming polymeric drug indomethacin-incorporated poly (ethylene oxide)-poly (β-benzyl L-aspartate) block copolymer micelles. J Pharm Sci. 1996;85(1):85-90. DOI: 10.1021/js950204r.
34. Parikh K, Singh S, Kumar S. Self assembly in an aqueous gemini surfactant containing sugar based (isosorbide) spacer. Arab J Chem. 2020;13(1): 1848-1857. DOI: 10.1016/j.arabjc.2018.01.020.
35. Wu W, Yao W, Wang X, Xie C, Zhang J, Jiang X. Bioreducible heparin-based nanogel drug delivery system. Biomaterials. 2015;39:260-268. DOI: 10.1016/j.biomaterials.2014.11.005.
36. Jeong YI, Nah JW, Lee HC, Kim SH, Cho CS. Adriamycin release from flower-type polymeric micelle based on star-block copolymer composed of poly(γ-benzyl l-glutamate) as the hydrophobic part and poly(ethylene oxide) as the hydrophilic part. Int J Pharm. 1999;188(1):49-58. DOI: 10.1016/S0378-5173(99)00202-1.
37. Ryu JG, Jeong YI, Kim IS, Lee JH, Nah JW, Kim SH. Clonazepam release from core-shell type nanoparticles of poly(ε-caprolactone)/poly(ethylene glycol)/poly(ε-caprolactone) triblock copolymers. Int J Pharm. 2000;200(2):231-242. DOI: 10.1016/S0378-5173(00)00392-6.
38. Gref R, Minamitake Y, Peracchia MT, Trubetskoy V, Torchilin V, Langer R. Biodegradable long-circulating polymeric nanospheres. Science. 1994;263(5153):1600-1603. DOI: 10.1126/science.8128245.
39. Jurczyk M, Jelonek K, Musiał-Kulik M, Beberok A, Wrześniok D, Kasperczyk J. Single-versus dual-targeted nanoparticles with folic acid and biotin for anticancer drug delivery. Pharmaceutics. 2021;13(3):326,1-38. DOI: 10.3390/pharmaceutics13030326.
40. Kumar P, Huo P, Liu B. Formulation strategies for folate-targeted liposomes and their biomedical applications. Pharmaceutics. 2019;11(8):381,1-28. DOI: 10.3390/pharmaceutics11080381.
41. Alam F, Al-Hilal TA, Chung SW, Park J, Mahmud F, Seo D, *et al*. Functionalized heparin-protamine based self-assembled nanocomplex for efficient anti-angiogenic therapy. J Control Release. 2015;197:180-9. DOI: 10.1016/j.jconrel.2014.11.009.
42. Alibolandi M, Abnous K, Hadizadeh F, Taghdisi SM, Alabdollah F, Mohammadi M, *et al*. Dextran-poly lactide-co-glycolide polymersomes decorated with folate-antennae for targeted delivery of docetaxel to breast adenocarcinima in vitro and in vivo. J Control Release. 2016;241:45-56. DOI: 10.1016/j.jconrel.2016.09.012.
43. Zamani M, Rostamizadeh K, Kheiri Manjili H, Danafar H. *In vitro* and *in vivo* biocompatibility study of folate-lysine-PEG-PCL as nanocarrier for targeted breast cancer drug delivery. European Polymer Journal. 2018;103:260-270. DOI: 10.1016/j.eurpolymj.2018.04.020.